

QCD analysis of light charged Higgs production through polarized top quark decay in two various frames

S. Mohammad Moosavi Nejad^{a,b*} and S. Abbaspour^a

^(a)Faculty of Physics, Yazd University, P.O. Box 89195-741, Yazd, Iran

^(b)School of Particles and Accelerators, Institute for Research in Fundamental Sciences (IPM), P.O.Box 19395-5531, Tehran, Iran

(Dated: September 13, 2018)

Light and heavy charged Higgs bosons are predicted by many models with an extended Higgs sector such as the two-Higgs-doublet model (2HDM). Searches for the charged Higgs bosons have been done by the ATLAS and the CMS experiments at the Large Hadron Collider (LHC) in proton-proton collision. However, a definitive search is a program that still has to be carried out so this belongs to the LHC experiments. The experimental observation of charged Higgs bosons would indicate physics beyond the Standard Model. In the present work we study the $\mathcal{O}(\alpha_s)$ correction to the energy spectrum of the inclusive bottom-flavored mesons (X_b) in polarized top quark decays into a light charged Higgs boson ($m_{H^\pm} < m_t$) and a massless bottom quark followed by $b \rightarrow X_b$ in the 2HDM, $t(\uparrow) \rightarrow H^\pm b \rightarrow H^\pm X_b + Jet$. This spin-dependent energy distribution is studied in two different helicity coordinate systems. This study could be considered as a new channel to search for the charged Higgs bosons at the LHC. To present our phenomenological predictions, we restrict ourselves to the unexcluded regions of the MSSM $m_{H^\pm} - \tan\beta$ parameter space determined by the recent results of the CMS and the ATLAS collaborations.

PACS numbers: 12.38.Bx, 13.85.Ni, 14.40.Nd, 14.65.Ha, 14.80.Da

I. INTRODUCTION

Charged Higgs bosons are predicted by several non-minimal Higgs scenarios [1], such as models including Higgs triplets [2] and two-Higgs-doublet models (2HDM) [3]. In the 2HDM, as a simplest model, the Higgs sector of the Standard Model (SM) is extended typically by adding an extra doublet of complex Higgs fields. In this model, after spontaneous symmetry breaking the particle spectrum includes five physical Higgs bosons: light and heavy CP-even Higgs bosons h and H with $m_H > m_h$, a CP-odd Higgs boson A , plus two charged Higgs bosons H^\pm [4]. The discovery of a charged Higgs boson would clearly indicate unambiguous evidence for the presence of new physics beyond the SM.

The production and decay modes of charged Higgs bosons depend on their masses, m_{H^\pm} . At hadron colliders, charged Higgs bosons can be produced through several channels. In a type-II 2HDM, which is the Higgs sector of the Minimal Supersymmetric Standard Model (MSSM) [5], the main production mode at the Large Hadron Collider (LHC) for light charged Higgs (with $m_{H^\pm} < m_t$) is through the top quark decay $t \rightarrow bH^\pm$. In this case, the light charged Higgses are produced most frequently via $t\bar{t}$ production. At the LHC, a cross section of $\sigma(pp \rightarrow t\bar{t}X) \approx 1$ (nb) is expected at design energy $\sqrt{S} = 14$ TeV [6]. With the LHC design luminosity of $10^{34} \text{cm}^{-2} \text{s}^{-1}$ in each of the four experiments, it is expected to produce about 90 million $t\bar{t}$ -pairs per year [7]. Thus, the LHC is a superlative top factory which lets

one to search for the charged Higgs bosons in the subsequent decay products of the top pairs $t\bar{t} \rightarrow H^\pm W^\mp b\bar{b}$ and $t\bar{t} \rightarrow H^\pm H^\mp b\bar{b}$ when H^\pm decays into τ -lepton and neutrino. For a review of all available production modes of light charged Higgs at the LHC, see also [8].

The combined Large Electron-Positron (LEP) experiments have determined a lower limit for the charged Higgs mass in a type-II 2HDM with $B(H^+ \rightarrow \tau\nu) = 1$ as $m_{H^+} > 94$ GeV [9], and the lower limit for any $B(H^+ \rightarrow \tau\nu)$ as 80 GeV. The experimental results from the Tevatron placed upper limits on $B(t \rightarrow H^+b)$ in the 15 – 20% range for light charged Higgs bosons. Both the CMS [10] and ATLAS [11, 12] collaborations searched for light charged Higgs bosons assuming $B(H^+ \rightarrow \tau\nu) = 1$ and improved the Tevatron limits to the 1 – 4% range for a mass range $m_{H^+} = 90 - 160$ GeV. We will discuss about the recent results on a search for the charged Higgs bosons by the CMS [13] and ATLAS [14] collaborations when we present our numerical analysis in Sec. IV.

The primary purpose of the present manuscript is the evaluation of the α_s -order QCD corrections to the differential decay width ($d\hat{\Gamma}/dx_i$) of a polarized top quark into a charged Higgs boson and a bottom quark, $t(\uparrow) \rightarrow bH^+$, where x_i is the scaled-energy fraction of the b-quark or the gluon emitted at the next-to-leading order (NLO). In the next section, we shall explain that to obtain the energy distribution of hadrons produced through the top decays in the MSSM, one needs these differential decay widths. The NLO QCD corrected decay distributions, $\Gamma(t \rightarrow bH^+)$, were previously computed in [15] for the polarized top quarks, and in [16–19] for the unpolarized ones. In Ref. [20], we calculated the unpolarized differential decay width $d\hat{\Gamma}(t \rightarrow bH^+)/dx_b$ at NLO and showed that our result after integration over x_b ($0 \leq x_b \leq 1$) is in

*Electronic address: mmoosavi@yazd.ac.ir

complete agreement with Refs. [16–18] and the corrected version of [19]. In [21], we studied the $\mathcal{O}(\alpha_s)$ radiative corrections to the spin-dependent differential decay rate of the process $t(\uparrow) \rightarrow bH^+$ in a special helicity coordinate system with the event plane defined in the (x, z) plane and the z -axis along the Higgs boson three-momentum (in the following called system 1). In this frame, the top quark polarization vector was measured with respect to the direction of the Higgs 3-momentum. We checked that our result was in complete agreement with the result presented in [15] after integration over x_b ($0 \leq x_b \leq 1$). Generally, to define the planes one needs to measure the momentum directions of the momenta \vec{p}_b and \vec{p}_{H^+} and the polarization direction of the top quark, where the measurement of the momentum direction of \vec{p}_b requires the use of a jet finding algorithm, whereas the polarization direction of the top quark must be obtained from the theoretical input. For example, in e^+e^- interactions the polarization degree of the top quark can be tuned with the help of polarized beams.

In the present work, we analyze the angular distribution of differential width of the process $t(\uparrow) \rightarrow bH^+$ in a different helicity coordinate system where, as before, the event plane is the (x, z) plane but with the z -axis along the bottom quark (in the following called system 2). In this system, the polarization direction of the top quark is evaluated with respect to the b-quark three-momentum (z -axis). This result is completely new. We also calculate the decay width $\Gamma(t(\uparrow) \rightarrow bH^+)$ in this new frame by integrating $d\Gamma/dx_b$ over $0 \leq x_b \leq 1$ and compare it with the previous result from [15].

On the other hand, bottom quarks produced through the top decays hadronize ($b \rightarrow X_b$) before they decay, therefore, each b-jet X_b contains a bottom-flavored hadron which most of the times is a B-meson. At the LHC, of particular interest is the distribution in the scaled-energy of B-mesons (x_B) produced through $t(\uparrow) \rightarrow BH^+ + X$ in the top quark rest frame. The study of these energy distributions in the polarized and unpolarized top decays could be proposed as a new channel to search for the charged Higgs bosons at the LHC. In [20], we studied the energy spectrum of the bottom-flavored mesons in unpolarized top quark decays into a charged Higgs boson and a bottom quark at NLO in the 2HDM. In [21] we studied the spin-dependent energy distribution of B-mesons produced through the polarized top decays at NLO in the helicity coordinate system 1. Here, our specific purpose is to study this angular correlation in a different helicity frame (system 2). Through this paper, we present our predictions for the B-meson energy spectrum in the polarized and unpolarized top decays and shall compare the polarized results in both helicity systems 1 and 2.

In the SM, due to the element $|V_{tb}| \approx 1$ of the Cabibbo-Kobayashi-Maskawa (CKM) [22] quark mixing matrix, the top quark decays dominantly through the two-body mode $t \rightarrow bW^+$. In [23–27], we investigated the energy distribution of B-mesons produced in polarized and un-

polarized top quark decays in the SM. In each top decay (polarized or unpolarized), to obtain the total distribution of the B-hadron energy two contributions due to the decay modes $t \rightarrow bH^+$ (in the 2HDM) and $t \rightarrow bW^+$ (in the SM) should be summed up. Although, the SM contribution is normally larger than the one coming from 2HDM [20].

This paper is organized as follows. In Sec. II, we study the inclusive production of a meson from polarized top quark considering the factorization theorem and DGLAP equations. In Sec. III, we present our analytical results of the $\mathcal{O}(\alpha_s)$ QCD corrections to the tree-level rate of $t(\uparrow) \rightarrow bH^+$. In Sec. IV, we present our numerical analysis of inclusive production of a meson from polarized top quark decay considering two different helicity coordinate systems. In Sec. V, our conclusions are summarized.

II. FORMALISM

In the proposed way to search for the light charged Higgs bosons, we study the inclusive production of a bottom-flavored meson (B) from polarized top quark decay in the following process

$$t(\uparrow) \rightarrow bH^+(g) \rightarrow H^+B + X, \quad (1)$$

where X stands for the unobserved final states and the gluon contributes to the real radiation at NLO. Both the b-quark and the gluon may hadronize into the B -meson.

If we label the four-momenta of top quark, b-quark, gluon and B -meson by p_t, p_b, p_g and p_B , respectively, then in the top quark rest frame the b-quark, gluon, and B-meson take energies $E_i = p_t \cdot p_i / m_t$ ($i = b, g, B$), where $m_B \leq E_B \leq (m_t^2 + m_B^2 - m_{H^+}^2) / (2m_t)$, $m_b \leq E_b \leq (m_t^2 + m_b^2 - m_{H^+}^2) / (2m_t)$ and $0 \leq E_g \leq (m_t^2 - (m_b + m_{H^+})^2) / (2m_t)$. Following Ref. [23], it is convenient to introduce the scaled energy fractions $x_i = E_i / E_b^{max} = 2E_i / (m_t(1 + R - y))$ ($i = b, g, B$) where the scaled masses y and R are defined as $y = m_{H^+}^2 / m_t^2$ and $R = m_b^2 / m_t^2$. By neglecting the b-quark mass m_b , one has $x_i = 2E_i / (m_t(1 - y))$ so that $0 \leq (x_b, x_g) \leq 1$.

In the first step, we analyze the parton-level sector of the decay process (1) in the rest frame of a top quark. The angular distribution of the differential decay width $d\hat{\Gamma}/dx_i$ ($i = b, g$) of a polarized top quark is given by the following simple expression to clarify the correlation between the polarization of the top quark and its decay products

$$\frac{d^2\hat{\Gamma}(t(\uparrow) \rightarrow bH^+(g))}{dx_i d \cos \theta_P} = \frac{1}{2} \left\{ \frac{d\hat{\Gamma}^{unpol}}{dx_i} \pm P \frac{d\hat{\Gamma}^{pol}}{dx_i} \cos \theta_P \right\}, \quad (2)$$

where P is the polarization degree of the top quark with $0 \leq P \leq 1$ so that $P = 1$ corresponds to 100% top quark polarization and $P = 0$ corresponds to an unpolarized top quark. In Eq. (2) $d\hat{\Gamma}^{unpol}/dx_i$ stands for the unpolarized differential rate, which is extensively calculated in [20] up to NLO, and $d\hat{\Gamma}^{pol}/dx_i$ refers to the polarized

one. The analytical expression for the differential partial width $d\hat{\Gamma}^{pol}/dx_i$ depends on the selected helicity coordinate system. In the rest frame of a top quark decaying into a b-quark, a Higgs boson and a gluon, the final state particles define an event plane. Relative to this plane, we can define the polarization direction of the polarized top quark. For the decay process (1), there are two various choices of possible coordinate systems relative to the event plane where one differentiates between frames according to the orientation of the z -axis.

In [21], we calculated the angular distribution of the partial decay width $d\hat{\Gamma}/dx_i$ in a specific frame (system 1) where the three-momentum of the charged Higgs boson (\vec{P}_{H^+}) pointed in the direction of the positive z -axis and the polar angle θ_P was defined as the angle between the polarization vector \vec{P}_t of the top quark and the positive z -axis. The sign '+' in (2) stands for this system.

Here, we consider a different helicity coordinate system (system 2) where the three-momentum of the bottom quark points in the direction of the positive z -axis (see Fig. 1). In (2), the sign '-' stands for the system 2. The technical detail of our calculation will be presented in the next section. We will show that the results depend on the selected helicity system.

Having the parton-level differential decay rates $d\hat{\Gamma}/dx_i$, our main purpose is to evaluate the distribution in the scaled-energy (x_B) of B-mesons in the polarized top quark rest frame. For this study, we evaluate the partial decay width of process (1) differential in x_B , $d\Gamma/dx_B$, at NLO where the normalized energy fraction of the B-meson is defined as $x_B = 2E_B/(m_t(1-y))$. According to the factorization theorem of the QCD-improved parton model [28], the energy distribution of a B-meson can be expressed as the convolution of the parton-level spectrum with the nonperturbative fragmentation function $D_i^B(z, \mu_F)$, describing the hadronization $i \rightarrow B$,

$$\frac{d\Gamma}{dx_B} = \sum_{i=b,g} \int_{x_i^{\min}}^{x_i^{\max}} \frac{dx_i}{x_i} \frac{d\hat{\Gamma}}{dx_i}(\mu_R, \mu_F) D_i^B\left(\frac{x_B}{x_i}, \mu_F\right), \quad (3)$$

where $d\hat{\Gamma}/dx_i (i = b, g)$ is the parton-level differential width of the process (1) in each selected helicity coordinate system. In the equation above, μ_F and μ_R are the factorization and the renormalization scales, respectively. In principle, one can use two different values for these scales; however, a choice often made consists of setting $\mu_R = \mu_F$ and we shall adopt this convention in our work. We will go back to the factorization theorem in Sec. IV, when our numerical analysis is presented.

In the next section, we present our analytic results for $d\hat{\Gamma}/dx_i (i = b, g)$ at NLO in the helicity system 2.

III. ANALYTIC RESULTS FOR $d\hat{\Gamma}/dx_i$

In this section we study the NLO radiative corrections to the partial decay width $t(\uparrow) \rightarrow b + H^+$ in the general

Figure 1: Polar angle θ_P defined in the second helicity coordinate system (system 2). \vec{P}_t stands for the top polarization vector in the top rest frame.

2HDM, where H_1 and H_2 are the doublets that their vacuum expectation values give masses to the down and up type quarks, respectively, and a linear combination of the charged components of H_1 and H_2 gives the physical charged Higgs H^\pm . In general models with two Higgs doublets and generic coupling to all the quarks, it is difficult to avoid tree-level flavor-changing neutral currents. We, thus, limit ourselves to the models that naturally stop these problems by restricting the Higgs coupling to all quarks. Generally, there are two possibilities (called two models in the following) for the two Higgs doublets to couple to the fermions. In these models, the relevant part of the interaction Lagrangian is expressed as [1]

$$L_I = \frac{g_W}{2\sqrt{2}m_W} V_{tb} H^+ [\bar{u}_t(p_t) \{A(1 + \gamma_5) + B(1 - \gamma_5)\} u_b(p_b)], \quad (4)$$

where A and B are model-dependent parameters and g_W is the weak coupling factor. In the first model (model I) the doublet H_1 couples to all bosons and the doublet H_2 couples to all the quarks. In this model, one has

$$A = m_t \cot \beta, \quad B = -m_b \cot \beta. \quad (5)$$

In the second model (model II), the doublet H_1 couples to the right-chiral down-type quarks and the doublet H_2 couples to the right-chiral up-type quarks. In this model, the interaction Lagrangian consists of

$$A = m_t \cot \beta, \quad B = m_b \tan \beta. \quad (6)$$

In (5) and (6), $\tan \beta = v_2/v_1$ is the ratio of the vacuum expectation values of the two electrically neutral components of the two Higgs doublets. These models are also known as type-I and type-II 2HDM scenarios.

In the following, we express the technical detail of our calculation for the Born-term rate, the virtual and real gluon corrections.

A. Born-level rate of $t \rightarrow bH^+$ in ZM-VFNS

The Born term amplitude in the MSSM for the process $t(\uparrow) \rightarrow b + H^+$ can either be expressed as a superposition of right- and left-chiral coupling factors, i.e.

$M_0 = \bar{u}_b\{g_t(1 + \gamma_5)/2 + g_b(1 - \gamma_5)/2\}u_t$, or as a superposition of scalar and pseudoscalar coupling factors, i.e. $M_0 = \bar{u}_b(a + b\gamma_5)u_t$, where $a = (g_t + g_b)/2$ and $b = (g_t - g_b)/2$. One also has $g_b = 2B$ and $g_t = 2A$ where A and B are defined in (5) and (6) for the models I and II. The inverse relation reads $a = A + B$ and $b = A - B$.

Therefore, for the Born amplitude squared one has: $|M_0|^2 = 2(p_b \cdot p_t)(a^2 + b^2) + 2(a^2 - b^2)m_b m_t + 4abm_t(p_b \cdot s_t)$ where we replaced $\sum_{s_t} u(p_t, s_t)\bar{u}(p_t, s_t) = (\not{p}_t + m_t)$ in the unpolarized Dirac string by $u(p_t, s_t)\bar{u}(p_t, s_t) = (1 - \gamma_5 \not{s}_t)(\not{p}_t + m_t)/2$ in the polarized state.

Considering Fig. 1, the polarization four-vector of the top quark in the top rest frame reads; $s_t = P(0; \sin\theta_P \cos\phi_P, \sin\theta_P \sin\phi_P, \cos\theta_P)$ and thus one has $p_b \cdot s_t = -P(|\vec{p}_b| \cos\theta_P)$. This justifies the minus sign in Eq. (2). Therefore, the tree-level helicity structure of differential rate reads

$$\frac{d^2\hat{\Gamma}_0}{dx_b d \cos\theta_P} = \frac{1}{2} \left\{ \hat{\Gamma}_0^{unpol} - P\hat{\Gamma}_0^{pol} \cos\theta_P \right\} \delta(1 - x_b), \quad (7)$$

where the unpolarized Born-level decay width is given by

$$\hat{\Gamma}_0^{unpol} = \frac{m_t(a^2 + b^2)}{16\pi} (1 + R - y) \times \lambda^{\frac{1}{2}}(1, R, y) \left\{ 1 + \frac{2\sqrt{R}}{1 + R - y} \left(\frac{a^2 - b^2}{a^2 + b^2} \right) \right\}, \quad (8)$$

and the polarized tree-level one, reads

$$\hat{\Gamma}_0^{pol} = \frac{m_t}{8\pi} \lambda(1, R, y)(ab), \quad (9)$$

where $\lambda(x, y, z) = x^2 + y^2 + z^2 - 2(xy + xz + yz)$ is the triangle function, $R = m_b^2/m_t^2$ and $y = m_{H^+}^2/m_t^2$. The above results are independent of the selected helicity frames and are in complete agreement with Refs. [15–19].

In the limit of vanishing b-quark mass ($m \rightarrow 0 \equiv R \rightarrow 0$) one has $a = b$ in the model I (or in the type-I 2HDM), then the tree-level decay width is simplified to

$$\hat{\Gamma}_0^{unpol} = \hat{\Gamma}_0^{pol} = \frac{m_t^3}{8\sqrt{2}\pi} G_F |V_{tb}|^2 (1 - y)^2 \cot^2 \beta, \quad (10)$$

and for the model II (type-II 2HDM), one has

$$\hat{\Gamma}_0^{unpol} = \frac{m_t^3}{8\sqrt{2}\pi} G_F |V_{tb}|^2 (1 - y)^2 \{ \cot^2 \beta + R \tan^2 \beta \} \times \left(1 + \frac{4R}{1 - y} \left(\frac{1}{\cot^2 \beta + R \tan^2 \beta} \right) \right), \quad (11)$$

and,

$$\hat{\Gamma}_0^{pol} = \frac{m_t^3}{8\sqrt{2}\pi} G_F |V_{tb}|^2 (1 - y)^2 \{ \cot^2 \beta - R \tan^2 \beta \}. \quad (12)$$

In (11) and (12), when the $R \tan^2 \beta$ -term can be compared with $\cot^2 \beta$ therefore one cannot naively set $m_b =$

0 in all expressions. For example, if we take $m_b = 4.78$ GeV, $m_t = 172.98$ GeV and from the unexcluded regions of the MSSM $m_{H^+} - \tan\beta$ parameter space [13, 14] we also take $m_{H^+} = 155$ GeV and $\tan\beta = 4$ thus the second term in the curly brackets in (11) and (12) can become as large as $\mathcal{O}(20\%)$ and this order will be larger when $\tan\beta$ is increased. Therefore, the $m_b \rightarrow 0$ approximation is not suitable for the type-II 2HDM. In this paper we work in the type-I 2HDM and adopt, with a very good approximation, the Born term presented in (10) in the massless or zero-mass variable-flavor-number (ZM-VFN) scheme [29] where the zero mass parton approximation is also applied to the bottom quark and the nonzero value of the b-quark mass only enter through the initial condition of the nonperturbative FF.

In the following, we present our analytical results for the $\mathcal{O}(\alpha_s)$ QCD corrections to the tree-level decay rate in the ZM-VFN scheme.

B. Virtual Corrections

The QCD virtual one-loop corrections to the polarized differential width arise from emission and absorption of a virtual gluon from the same quark leg (quark self-energy) and from a virtual gluon exchanged between the top and bottom quark legs (vertex correction). In the ZM-VFN scheme all divergences including the infrared (IR) and ultra-violet (UV) singularities which arise from the collinear- and the soft-gluon emissions, respectively, are regularized by dimensional regularization in $D = 4 - 2\epsilon$ space-time dimensions to become single poles in ϵ . These singularities are subtracted at factorization scale μ_F and absorbed into the bare FFs according to the modified minimal-subtraction scheme (\overline{MS}). The virtual contributions are the same in both helicity systems 1 and 2, and more detail of our calculation can be found in [21]. We just mention that by neglecting the b-quark mass the counter term of the vertex consists of the top quark mass renormalization and the wave function renormalizations of both top and bottom quarks. Here, we just present our final result of the virtual corrections to the polarized differential decay rate as

$$\frac{d\hat{\Gamma}^{vir,pol}}{dx_b} = \hat{\Gamma}_0^{pol} \frac{\alpha_s(\mu_R)}{2\pi} C_F \delta(1 - x_b) \left(-\frac{1}{\epsilon^2} + \frac{F}{\epsilon} - \frac{F^2}{2} + \left(\frac{2}{y} - 5 \right) \ln(1 - y) - 2Li_2(y) - \frac{7}{8} - \frac{\pi^2}{12} \right), \quad (13)$$

where, $F = 2 \ln(1 - y) - \ln(4\pi\mu_F^2/m_t^2) + \gamma_E - 5/2$, $C_F = (N_c^2 - 1)/(2N_c) = 4/3$ for $N_c = 3$ quark colors, and $Li_2(x) = -\int_0^x (dt/t) \ln(1 - t)$ is the Spence function. Note that, all UV-divergences are canceled after summing all virtual corrections up but the IR-singularities are remaining which are labeled by ϵ in the above equation. Since the virtual corrections are the same in both helicity systems 1 and 2, the above result is in agreement with

[15] where the authors have considered the first helicity system.

C. Real gluon Corrections

In this section we calculate the $\mathcal{O}(\alpha_s)$ QCD corrections (i.e. $t(\uparrow) \rightarrow bH^+g$) which are needed to cancel the IR-singularities of the virtual corrections. In the rest frame of a top quark decaying into a Higgs boson, a bottom quark and a gluon the outgoing particles define an event plane so that relative to this plane one can define the spin direction of the polarized top quark. For our aim, two possible coordinate systems are defined as

$$\begin{aligned} \text{System 1} &: \vec{p}_{H^+} \parallel \hat{z}; (\vec{p}_b)_x \geq 0 \\ \text{System 2} &: \vec{p}_b \parallel \hat{z}; (\vec{p}_{H^+})_x \geq 0 \end{aligned} \quad (14)$$

The various helicity systems provide independent probes of light charged Higgs bosons in the polarized top quark decay dynamics.

In [21], we analyzed the spin-momentum correlation between the top quark polarization vector and the momenta of its decay products in the system 1. In the present work, we study the same analysis in the system 2 and show that the energy spectrum of the outgoing B-meson depends on the helicity system selected. Considering the general form of angular distribution of the differential decay width (2), one has

$$\frac{d^2\hat{\Gamma}^{real}}{dx_b d\cos\theta_P} = \frac{1}{2} \left(\frac{d\hat{\Gamma}^{unpol,real}}{dx_b} - P \frac{d\hat{\Gamma}^{pol,real}}{dx_b} \cos\theta_P \right), (15)$$

where $d\hat{\Gamma}^{unpol}/dx_b$ is presented in [20].

The $\mathcal{O}(\alpha_s)$ real gluon (tree-graph) contribution to the differential decay rate results from the square of the real amplitude as $|M^{\text{real}}|^2 = M^{\text{real}\dagger} \cdot M^{\text{real}}$, where M^{real} reads

$$\begin{aligned} M^{\text{real}} &= g_s \frac{\lambda^a}{2} \bar{u}(p_b, s_b) \left\{ \frac{2p_t^\mu - \not{p}_g \gamma^\mu}{2p_t \cdot p_g} \right. \\ &\quad \left. - \frac{2p_b^\mu + \gamma^\mu \not{p}_g}{2p_b \cdot p_g} \right\} (a\mathbf{1} + b\gamma_5) u(p_t, s_t) \epsilon_\mu^*(p_g, r), \end{aligned} \quad (16)$$

where the polarization vector of the real gluon with the momentum p_g and spin r is denoted by $\epsilon(p_g, r)$. The first and second terms in the curly brackets refer to the real gluon emission from the top and the bottom quarks, respectively.

As before, to regulate the IR-divergences we work in $D = 4 - 2\epsilon$ dimensions, therefore from the definition of decay rate, one has

$$d\hat{\Gamma}^{real} = \frac{\mu_F^{2(4-D)}}{2m_t} |M^{\text{real}}|^2 dPS(p_t, p_b, p_g, p_{H^+}), \quad (17)$$

where, the Phase Space element reads

$$\begin{aligned} dPS &= \frac{d^{D-1}\mathbf{p}_b}{(2\pi)^{D-1}2E_b} \frac{d^{D-1}\mathbf{p}_{H^+}}{(2\pi)^{D-1}2E_{H^+}} \frac{d^{D-1}\mathbf{p}_g}{(2\pi)^{D-1}2E_g} \\ &\quad \times (2\pi)^D \delta^D(p_t - p_b - p_{H^+} - p_g). \end{aligned} \quad (18)$$

To calculate the real polarized differential decay rate $d\hat{\Gamma}^{pol,real}/dx_b$, we fix the momentum of the bottom quark in Eq. (17) and integrate over the gluon energy which ranges as $m_t S(1-x_b) \leq E_g \leq m_t S(1-x_b)/(1-2Sx_b)$ where $S = (1-y)/2$. Also, to get the correct finite terms one has to normalize it to the Born width (10) which is evaluated in the dimensional regularization at $\mathcal{O}(\epsilon^2)$, i.e. $\hat{\Gamma}_0^{pol} \rightarrow \hat{\Gamma}_0^{pol} \{1 - \epsilon(\gamma_E + 2\ln S - \ln(4\pi\mu_F^2/m_t^2))\}$. Thus, in the second helicity coordinate system the contribution of the real gluon emission into the normalized differential decay width is given by

$$\begin{aligned} \frac{1}{\hat{\Gamma}_0^{pol}} \frac{d\hat{\Gamma}^{real,pol}}{dx_b} &= \frac{\alpha_s}{2\pi} C_F \left\{ \delta(1-x_b) \left[\frac{1}{\epsilon^2} - \frac{1}{\epsilon} \left(F + \frac{3}{2} \right) + \frac{F^2}{2} \right. \right. \\ &\quad \left. \left. + \frac{3}{2} F - 2 \frac{y}{1-y} \ln y + 2Li_2(1-y) - \frac{\pi^2}{4} \right. \right. \\ &\quad \left. \left. + \frac{5}{8} \right] + \frac{1+x_b^2}{(1-x_b)_+} \left[-\frac{1}{\epsilon} + 2\ln x_b + F \right. \right. \\ &\quad \left. \left. + \frac{3}{2} \right] + 2(1+x_b^2) \left(\frac{\ln(1-x_b)}{1-x_b} \right)_+ \right\}, \end{aligned} \quad (19)$$

where $F = 2\ln(1-y) - \ln(4\pi\mu_F^2/m_t^2) + \gamma_E - 5/2$ and the plus distributions are defined as usual.

D. Analytic Results for Partial Decay Rates $d\hat{\Gamma}/dx_i$ in the helicity system 2

The NLO expression for the $d\hat{\Gamma}^{pol}/dx_b$ is obtained by summing the Born term, the virtual one-loop and the real gluon contributions. Our result for the helicity coordinate system 2, is as follows

$$\begin{aligned} \frac{d\hat{\Gamma}^{pol}}{dx_b} &= \hat{\Gamma}_0^{pol} \left\{ \delta(1-x_b) + \frac{\alpha_s(\mu_R)}{2\pi} \left\{ \left[-\frac{1}{\epsilon} + \gamma_E - \ln 4\pi \right] \right. \right. \\ &\quad \times P_{qq}^{(0)}(x_b) + C_F \left[\delta(1-x_b) \left[2 \frac{1-y}{y} \ln(1-y) \right. \right. \\ &\quad \left. \left. - 4 - \frac{2y}{1-y} \ln y - \frac{\pi^2}{3} - 2Li_2(y) + 2Li_2(1-y) \right. \right. \\ &\quad \left. \left. - \frac{3}{2} \ln \frac{\mu_F^2}{m_t^2} \right] - \frac{1+x_b^2}{(1-x_b)_+} \left[1 - 2\ln(x_b(1-y)) \right. \right. \\ &\quad \left. \left. + \ln \frac{\mu_F^2}{m_t^2} \right] + 2(1+x_b^2) \left(\frac{\ln(1-x_b)}{1-x_b} \right)_+ \right\} \right\}, \end{aligned} \quad (20)$$

where $P_{qq}^{(0)}$ is the time-like $q \rightarrow q$ splitting function at leading order [30], so

$$P_{qq}^{(0)}(x_b) = C_F \left(\frac{1+x_b^2}{(1-x_b)_+} + \frac{3}{2} \delta(1-x_b) \right). \quad (21)$$

Since, the bottom-flavored hadrons can be also produced through the hadronization of the emitted real gluon at NLO, we also need the differential decay rate $d\hat{\Gamma}^{pol}/dx_g$ in the ZM-VFN scheme. To calculate the

$d\hat{\Gamma}^{pol}/dx_g$ we start from Eq. (17) and fix the momentum of the gluon and integrate over the bottom quark energy so that $m_t S(1-x_g) \leq E_b \leq m_t S(1-x_g)/(1-2Sx_g)$. Since we fix the gluon momentum, then there will be no soft singularities in the $d\hat{\Gamma}^{pol}/dx_g$. The result in the helicity system 2, reads

$$\begin{aligned} \frac{d\hat{\Gamma}^{pol}}{dx_g} &= \hat{\Gamma}_0^{pol} \left\{ \frac{\alpha_s(\mu_R)}{2\pi} \left\{ \left[-\frac{1}{\epsilon} + \gamma_E - \ln 4\pi \right] \times P_{gq}^{(0)}(x_g) \right. \right. \\ &\quad + C_F \left[3 - \frac{y^2}{4S(1-2Sx_g)^2} + \frac{1}{Sx_g^2} \ln(1-2Sx_g) \right. \\ &\quad + \frac{12S^2 - 8S + 1}{4S(1-2Sx_g)} - \frac{x_g}{2} - \frac{1 + (1-x_g)^2}{x_g} \left(\ln \frac{\mu_F^2}{m_t^2} \right. \\ &\quad \left. \left. \left. - \ln \frac{4S^2 x_g^2 (1-x_g)^2}{1-2Sx_g} \right) \right] \right\} \right\}, \end{aligned} \quad (22)$$

where $P_{gq}^{(0)}$ is the time-like $q \rightarrow g$ splitting function at LO [30],

$$P_{gq}^{(0)}(x_g) = C_F \left(\frac{1 + (1-x_g)^2}{x_g} \right). \quad (23)$$

To subtract the collinear singularities remaining in Eqs. (20) and (22), we apply the modified minimal subtraction (\overline{MS}) scheme where the collinear singularities are absorbed into the bare FFs. This renormalizes the FFs and generates the finite terms of the form $\alpha_s \ln(m_t^2/\mu_F^2)$ in the polarized differential decay rates. According to this scheme, in order to get the \overline{MS} coefficient functions we shall have to subtract from Eqs. (20) and (22) the $\mathcal{O}(\alpha_s)$ term multiplying the characteristic \overline{MS} constant $(-1/\epsilon + \gamma_E - \ln 4\pi)$. In this work we set $\mu_R = \mu_F = m_t$, so that in Eqs. (20) and (22) the terms proportional to $\ln(m_t^2/\mu_F^2)$ vanish.

Integrating $d\hat{\Gamma}^{pol}/dx_b$ of Eq. (20) over $x_b(0 < x_b < 1)$, we obtain the NLO renormalized decay rate as

$$\begin{aligned} \hat{\Gamma}^{pol} &= \hat{\Gamma}_0^{pol} \left\{ 1 - \frac{C_F \alpha_s}{2\pi} \left[\frac{2y}{1-y} \ln y + (5 - \frac{2}{y}) \ln(1-y) + \right. \right. \\ &\quad \left. \left. 2Li_2(y) - 2Li_2(1-y) - \frac{7}{2} + \pi^2 \right] \right\}. \end{aligned} \quad (24)$$

Our previous result for $\hat{\Gamma}^{pol}(= \int_0^1 dx_b d\hat{\Gamma}^{pol}/dx_b)$ in the helicity system 1 [21] was in complete agreement with Ref. [15], but the above result computed in the second frame (system 2) is completely new.

IV. NUMERICAL ANALYSIS IN TYPE-I 2HDM

In the MSSM, the mass of charged Higgs bosons is restricted by $m_{H^\pm} > m_{W^\pm}$ at tree-level [31], but this restriction does not hold for some regions of parameter space after including radiative corrections. In this model, m_{H^\pm} is strongly correlated with the mass of other Higgs bosons. In [16], it is mentioned that a charged Higgs

boson with a mass range $80 \text{ GeV} \leq m_{H^\pm} \leq 160 \text{ GeV}$ is a logical possibility and its effects should be searched for in the decay mode $t \rightarrow bH^+ \rightarrow B\tau^+\nu_\tau + X$. On the other hand, the recent results of a search for evidence of a charged Higgs boson in $19.5-19.7 \text{ fb}^{-1}$ of proton-proton collision data recorded at $\sqrt{s} = 8 \text{ TeV}$ are reported by the CMS [13] and the ATLAS [14] collaborations, using the $\tau + jets$ channel with a hadronically decaying τ lepton in the final state. According to Fig. 7 of Ref. [14], the large region in the MSSM $m_{H^+} - \tan\beta$ parameter space is excluded for $m_{H^+} = 80-160 \text{ GeV}$. So, the unexcluded regions of this parameter space include the charged Higgs masses as $90 \leq m_{H^+} \leq 100 \text{ GeV}$ (with $6 < \tan\beta < 10$) and $140 \leq m_{H^+} \leq 160 \text{ GeV}$ (with $3 < \tan\beta < 21$). See also Fig. 9 of Ref. [13]. Therefore, these values of m_{H^\pm} and $\tan\beta$ are still allowed and in this work our prediction and analysis is restricted to these regions. However, a definitive search of the charged Higgs bosons over this part of the $m_{H^+} - \tan\beta$ parameter space is a program that still has to be carried out and this belongs to the LHC experiments.

Here, for our numerical analysis we adopt the input parameter values from Ref. [31] as; $G_F = 1.16637 \times 10^{-5} \text{ GeV}^{-2}$, $m_t = 172.98 \text{ GeV}$, $m_b = 4.78 \text{ GeV}$, $m_W = 80.399 \text{ GeV}$, $m_B = 5.279 \text{ GeV}$, and $|V_{tb}| = 0.999152$. Considering the unexcluded $m_{H^+} - \tan\beta$ parameter space from the ATLAS experiments [14], we also consider $m_{H^+} = 95, 155 \text{ GeV}$ and 160 GeV .

In the ZM-VFN scheme the polarized and unpolarized decay rates at the Born level are the same in both helicity systems (see (10) and corresponding explanation) and from now we label them by $\hat{\Gamma}_0 (= \hat{\Gamma}_0^{unpol} = \hat{\Gamma}_{1,0}^{pol} = \hat{\Gamma}_{2,0}^{pol})$. Our result for the unpolarized rate at NLO, is

$$\begin{aligned} \hat{\Gamma}^{unpol} &= \hat{\Gamma}_0(1 - 0.010) \quad , \quad \text{for } m_{H^+} = 160 \text{ GeV} \\ \hat{\Gamma}^{unpol} &= \hat{\Gamma}'_0(1 - 0.028) \quad , \quad \text{for } m_{H^+} = 155 \text{ GeV} \\ \hat{\Gamma}^{unpol} &= \hat{\Gamma}''_0(1 - 0.086) \quad , \quad \text{for } m_{H^+} = 95 \text{ GeV} \end{aligned}$$

and for the polarized rate in the system 1, one has

$$\begin{aligned} \hat{\Gamma}_1^{pol} &= \hat{\Gamma}_0(1 - 0.037) \quad , \quad \text{for } m_{H^+} = 160 \text{ GeV} \\ \hat{\Gamma}_1^{pol} &= \hat{\Gamma}'_0(1 - 0.038) \quad , \quad \text{for } m_{H^+} = 155 \text{ GeV} \\ \hat{\Gamma}_1^{pol} &= \hat{\Gamma}''_0(1 - 0.043) \quad , \quad \text{for } m_{H^+} = 95 \text{ GeV} \end{aligned}$$

and for the NLO polarized width in the helicity system 2, we have

$$\begin{aligned} \hat{\Gamma}_2^{pol} &= \hat{\Gamma}_0(1 - 0.033) \quad , \quad \text{for } m_{H^+} = 160 \text{ GeV} \\ \hat{\Gamma}_2^{pol} &= \hat{\Gamma}'_0(1 - 0.051) \quad , \quad \text{for } m_{H^+} = 155 \text{ GeV} \\ \hat{\Gamma}_2^{pol} &= \hat{\Gamma}''_0(1 - 0.109) \quad , \quad \text{for } m_{H^+} = 95 \text{ GeV} \end{aligned}$$

In the above results the $\hat{\Gamma}_0$, $\hat{\Gamma}'_0$ and $\hat{\Gamma}''_0$ depend on the m_{H^+} and $\tan\beta$, see (10). As is seen, the NLO polarized decay rates depend on the selected helicity coordinate system. In obtaining the results above, we applied the unpolarized decay rate presented in [20] and the polarized

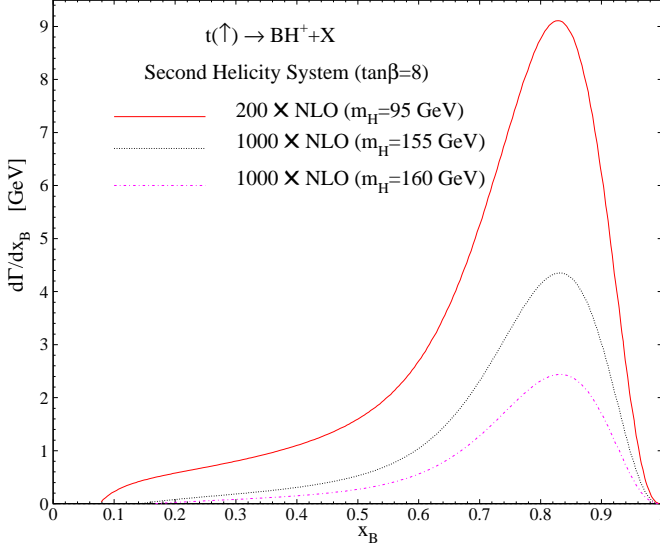


Figure 2: The NLO x_B -spectrum ($d\Gamma/dx_B$) in polarized top decay in the helicity coordinate system 2 with $\tan\beta = 8$ and $m_{H^+} = 95$ GeV (solid line), $m_{H^+} = 155$ (dotted line) and 160 GeV (dot-dashed line).

ones in the first and second helicity systems given in [21] and (24), respectively.

After our numerical analysis of decay widths we are now in a situation to present our phenomenological predictions for the scaled-energy (x_B) spectrum of bottom-flavored mesons (B) inclusively produced in polarized top decays in the type-I 2HDM. To show our predictions for the x_B -distribution, we consider the doubly differential distribution $d^2\Gamma/(dx_B d\cos\theta_P)$ of the partial width of the decay $t(\uparrow) \rightarrow BH^+ + X$ in the system 2. Here, $x_B = 2E_B/(m_t(1-y))$ is the scaled-energy fraction of the B-meson in the top quark rest frame, where the energy of B-meson ranges from $E_B^{min} = m_B$ to $E_B^{max} = (m_t^2 + m_B^2 - m_{H^+}^2)/(2m_t)$.

According to the factorization formula (3), the required ingredients for this study are the parton-level differential decay widths (20) and (22) and the fragmentation functions (FFs) $D_b^B(z)$ and $D_g^B(z)$ which describe the splitting of $b \rightarrow B$ and $g \rightarrow B$, respectively. To describe these hadronization processes, from Ref. [32] we employ the nonperturbative B-hadron FFs determined at NLO in the ZM-VFN scheme through a global fit to e^+e^- annihilation data taken by OPAL [33], ALEPH [34] and SLD [35]. In Ref. [32] authors used a simple power model $D_b(z, \mu_F^{ini}) = Nz^\alpha(1-z)^\beta$ as the initial condition for the $b \rightarrow B$ FF at $\mu_F^{ini} = 4.5$ GeV, while the gluon and light-quark FFs were generated via the DGLAP evolution equations [30]. The fit yielded the values $N = 4684.1$, $\alpha = 16.87$, and $\beta = 2.628$ for the FF parameters.

Considering the unexcluded $m_{H^+} - \tan\beta$ parameter space from the CMS [13] and the ATLAS [14] experiments, in Fig. 2 we show our prediction for the x_B -spectrum at NLO in the system 2, taking $m_{H^+} = 95$ GeV

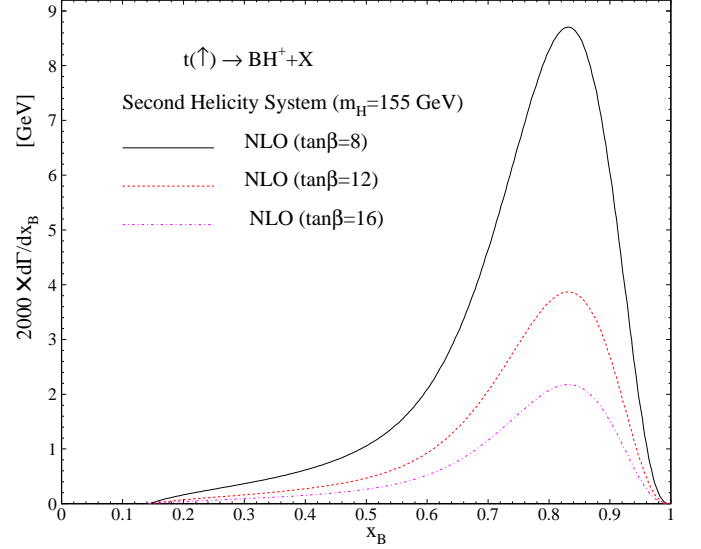


Figure 3: x_B spectrum in polarized top decay in the type-I 2HDM with different values of $\tan\beta = 8, 12$ and 16. The charged Higgs boson mass is set to $m_{H^+} = 155$ GeV. Analysis is done in the second helicity coordinate system.

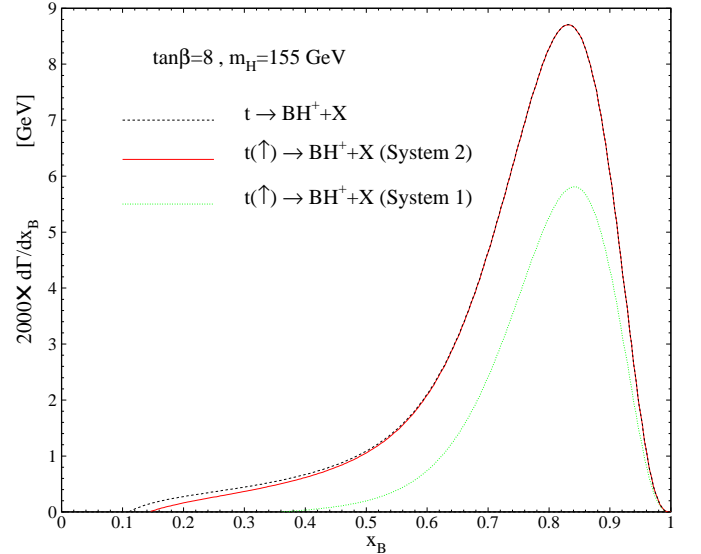


Figure 4: $d\Gamma/x_B$ as a function of x_B in the type-I 2HDM considering the ZM-VFN scheme. The unpolarized (dashed line) and polarized partial decay rates are compared at NLO taking $m_{H^+} = 155$ GeV, $\tan\beta = 8$ and $\mu_R = \mu_F = m_t$. For the polarized top decays we used the helicity system 1 (dotted line) and 2 (solid line). Details are discussed in the text.

(solid line), $m_{H^+} = 155$ GeV (dotted line) and $m_{H^+} = 160$ GeV (dot-dashed line) where $\tan\beta = 8$ is fixed for all predictions. As is seen, when m_{H^+} increases the size of decay rate decreases but the peak position is shifted towards higher values of x_B .

Considering the results of the CMS [13] and ATLAS [14] experiments where $4 \leq \tan\beta \leq 16$ is allowed for

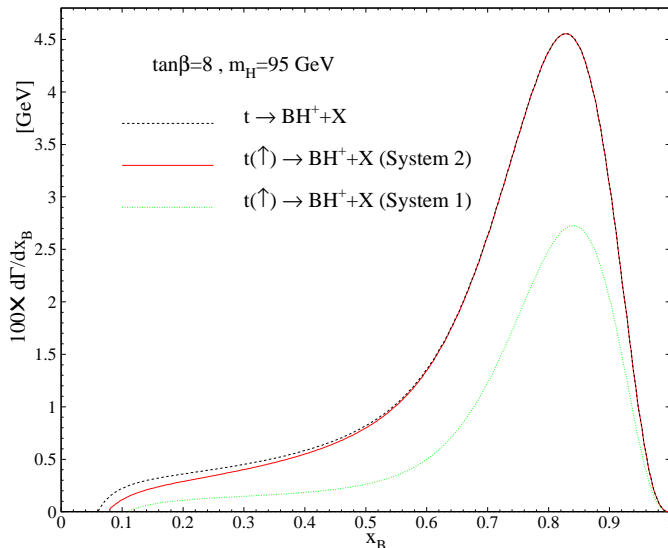


Figure 5: As in Fig. 4, but for $m_{H^+} = 95$ GeV. This mass is not excluded by the ATLAS experiments [14].

$m_{H^+} = 155$ GeV, in Fig. 3 we study the energy spectrum of B-meson in the helicity system 2 for different values of $\tan\beta = 8$ (solid line), 12 (dashed line) and 16 (dot-dashed line), where the mass of Higgs boson is set to $m_{H^+} = 155$ GeV for all analysis. As is seen, when $\tan\beta$ increases the size of decay rate decreases. This is obvious because $\hat{\Gamma}_0$ (10) is proportional to $\cot^2\beta$.

In Fig. 4, taking $m_{H^+} = 155$ GeV and $\tan\beta = 8$ the NLO energy spectrum of B-mesons from polarized top decays, $t(\uparrow) \rightarrow BH^+ + X$, in the first (dotted line) and second (solid line) helicity coordinate systems are shown. As is seen the energy distributions obtained from our analysis in two various systems are different and the size of NLO correction is larger in the system 2. For more comparison, we also plotted the energy distribution of B-mesons through unpolarized top quark decays (dashed line). A considerable point is that the size of NLO corrections is the same both for the polarized top decay in the helicity system 2 and for the unpolarized one, except for small values of x_B ($0.14 < x_B < 0.45$). In this region the unpolarized distribution is larger.

In Fig. 5, as in Fig. 4, the same comparisons are done but for $m_{H^+} = 95$ GeV. Our results show that in these cases the NLO corrections are similar in the shape, however, the unpolarized distribution shows a more enhancement in size at NLO.

It should be pointed out that our formalism elaborated here can be also extended to the production of hadron species other than bottom-flavored hadrons, such as pions, kaons and protons, etc., using the nonperturbative $(b, g) \rightarrow \pi/K/P$ FFs extracted in our recent works [36, 37], relying on their universality and scaling violations [38].

V. CONCLUSIONS

Charged Higgs bosons (H^\pm) are predicted in models consisting of at least two Higgs doublets, of which the simplest are the two-Higgs-doublet models (2HDM). The charged-Higgses have been searched for in high energy experiments, in particular, at the Tevatron, ATLAS and CMS but they have not been seen so far. The discovery of a charged Higgs would represent unambiguous evidence for the presence of physics beyond the SM.

In the 2HDM, the main production mode of light charged Higgs boson ($m_{H^+} < m_t$) is through the top quark decay, $t \rightarrow bH^+$. On the other hand, bottom quarks hadronize, via $b \rightarrow B + X$, before they decay, so that the decay process $t \rightarrow BH^+ + X$ is of prime importance at the LHC. Therefore, the study of scaled-energy (x_B) distribution of the bottom-flavored mesons (B) inclusively produced in top quark decays is proposed as a new way to search for the light charged Higgs bosons. For this study, we need to evaluate the quantity $d\Gamma/dx_B$.

In [20], we studied the energy spectrum of the B-mesons in unpolarized top decays into a charged-Higgs boson and a b-quark at NLO in the 2HDM. In [21] we studied the spin-dependent energy distribution of B-mesons produced through the polarized top decays at NLO in a special helicity coordinate system (system 1), where the event plane lied in the (x, z) plane and the Higgs three-momentum was along the z -axis. In the present work, we have presented results on the NLO radiative corrections to the spin-dependent differential width $d^2\Gamma/(dx_B d\cos\theta_P)$, applying a different helicity system (system 2) where the z -axis is defined by the b-quark 3-momentum. This provides an independent probe of charged Higgses. To make these predictions we obtained the analytical results for the parton-level differential decay width $d\hat{\Gamma}(t(\uparrow) \rightarrow bH^+(+g))/dx_a$ ($a = b, g$) in two helicity systems 1 and 2. Our result for the unpolarized differential decay width $d\hat{\Gamma}(t \rightarrow bH^+)/dx_b$ was in complete agreement with Refs. [16–19] after integration over $0 \leq x_b \leq 1$, and our result for the polarized one in the system 1 was in agreement with [15] after integration over x_b . Here, using the same techniques we calculated the polarized differential width in the helicity system 2 and we also computed, for the first time, the polarized rate in the system 2. We found that the polarized results depend on the selected helicity system, extremely.

For our numerical analysis, considering the recent results reported by the CMS [13] and ATLAS [14] collaborations we restricted ourselves to the unexcluded regions of the MSSM $m_{H^+} - \tan\beta$ parameter space which include $90 \leq m_{H^+} \leq 100$ GeV (with $6 < \tan\beta < 10$) and $140 \leq m_{H^+} \leq 160$ GeV (with $3 < \tan\beta < 21$).

VI. ACKNOWLEDGMENTS

We would like to thank the CERN TH-PH division for its hospitality where a portion of this work was per-

formed.

-
- [1] J. F. Gunion, H. Haber, G. Kane, and S. Dawson, *The Higgs Hunter's Guide* (Addison-Wesley, Reading, MAA, 1990), and references therein.
- [2] T. P. Cheng and L. F. Li, Phys. Rev. D **22** (1980) 2860.
- [3] T. D. Lee, Phys. Rev. D **8** (1973) 1226.
- [4] A. Djouadi, Phys. Rept. **459** (2008) 1.
- [5] K. Inoue, A. Kakuto, H. Komatsu and S. Takeshita, Prog. Theor. Phys. **68** (1982) 927; Erratum: [Prog. Theor. Phys. **70** (1983) 330].
- [6] U. Langenfeld, S. Moch and P. Uwer, arXiv:0907.2527 [hep-ph].
- [7] S. Moch and P. Uwer, Phys. Rev. D **78** (2008) 034003; N. Kidonakis and R. Vogt, Phys. Rev. D **78** (2008) 074005.
- [8] M. Aoki, R. Guedes, S. Kanemura, S. Moretti, R. Santos and K. Yagyu, Phys. Rev. D **84** (2011) 055028.
- [9] G. Abbiendi *et al.* [ALEPH and DELPHI and L3 and OPAL and LEP Collaborations], Eur. Phys. J. C **73** (2013) 2463.
- [10] S. Chatrchyan *et al.* [CMS Collaboration], JHEP **1207** (2012) 143.
- [11] G. Aad *et al.* [ATLAS Collaboration], JHEP **1206** (2012) 039.
- [12] G. Aad *et al.* [ATLAS Collaboration], JHEP **1303** (2013) 076.
- [13] CMS Collaboration [CMS Collaboration], CMS-PAS-HIG-14-020.
- [14] The ATLAS collaboration [ATLAS Collaboration], ATLAS-CONF-2013-090.
- [15] A. Kadeer, J. G. Körner, and M. C. Mauser, Eur. Phys. J. C **54**, 175 (2008).
- [16] A. Ali, E. A. Kuraev and Y. M. Bystritskiy, Eur. Phys. J. C **67**, 377 (2010).
- [17] A. Czarnecki and S. Davidson, Phys. Rev. D **47**, 3063 (1993).
- [18] J. Liu and Y. P. Yao, Phys. Rev. D **46**, 5196 (1992).
- [19] C. S. Li and T. C. Yuan, Phys. Rev. D **42** (1990) 3088; Erratum: [Phys. Rev. D **47** (1993) 2156].
- [20] S. M. Moosavi Nejad, Phys. Rev. D **85** (2012) 054010; Eur. Phys. J. C **72** (2012) 2224.
- [21] S. M. Moosavi Nejad and S. Abbaspour, arXiv:1610.03811 [hep-ph].
- [22] N. Cabibbo, Phys. Rev. Lett. **10**, 531 (1963); M. Kobayashi and T. Maskawa, Prog. Theor. Phys. **49**, 652 (1973).
- [23] B. A. Kniehl, G. Kramer and S. M. Moosavi Nejad, Nucl. Phys. B **862** (2012) 720.
- [24] S. M. Moosavi Nejad, Phys. Rev. D **88** (2013) no.9, 094011.
- [25] S. M. Moosavi Nejad and M. Balali, Phys. Rev. D **90** (2014) no.11, 114017.
- [26] S. M. Moosavi Nejad, Nucl. Phys. B **905** (2016) 217.
- [27] S. M. Moosavi Nejad and M. Balali, Eur. Phys. J. C **76** (2016) no.3, 173.
- [28] J. C. Collins, Phys. Rev. D **66** (1998) 094002.
- [29] J. Binnewies, B. A. Kniehl and G. Kramer, Phys. Rev. D **58**, 034016 (1998).
- [30] V. N. Gribov and L. N. Lipatov, Sov. J. Nucl. Phys. **15**, 438 (1972) [Yad. Fiz. **15**, 781 (1972)]; G. Altarelli and G. Parisi, Nucl. Phys. **B126**, 298 (1977); Yu. L. Dokshitzer, Sov. Phys. JETP **46**, 641 (1977) [Zh. Eksp. Teor. Fiz. **73**, 1216 (1977)].
- [31] K. Nakamura *et al.* (Particle Data Group), J. Phys. G **37**, 075021 (2010).
- [32] B. A. Kniehl, G. Kramer, I. Schienbein, and H. Spiesberger, Phys. Rev. D **77**, 014011 (2008).
- [33] G. Abbiendi *et al.* (OPAL Collaboration), Eur. Phys. J. C **29**, 463 (2003).
- [34] A. Heister *et al.* (ALEPH Collaboration), Phys. Lett. B **512**, 30 (2001).
- [35] K. Abe *et al.* (SLD Collaboration), Phys. Rev. Lett. **84**, 4300 (2000); Phys. Rev. D **65**, 092006 (2002); **66**, 079905 (2002).
- [36] M. Soleymaninia, A. N. Khorramian, S. M. Moosavi Nejad and F. Arbabifar, Phys. Rev. D **88** (2013) no.5, 054019.
- [37] S. M. Moosavi Nejad, M. Soleymaninia and A. Maktoubian, Eur. Phys. J. A **52** (2016) no.10, 316.
- [38] J. C. Collins, Phys. Rev. D **58**, 094002 (1998).